TRANSIENT HEATING OF A PACKED BED COMPRISING TWO DIFFERENT REFRACTORY MATERIALS

***E. Resendiz-Mora[1], V. Dupont[1], T. Mahmud[1], P. J. Heggs[1]**

[1]School of Chemical and Process Engineering, University of Leeds, Leeds LS2 9JT, United Kingdom

1. INTRODUCTION

The transition towards more sustainable energy use and production relates to the ability of recovering as much heat as possible and to provide storage to handle the heat available from waste streams or that generated from renewables. Packed beds can be used as heat sinks to store energy and help spreading the use of renewables [1, 2]. Meanwhile, new concepts to enhance the integration of heat are being studied. This is the case of fixed bed reactors packed with multiple refractory materials acting as sink or source of energy [3]. Models of these type of systems have so far been addressed considering a pseudo-homogeneous behaviour [4], thus discarding the inter-pellet and intra-pellet thermal resistances to heat transfer. This might prove unrealistic, and, in this discourse, we develop a modelling framework for the heat transfer model without considering heat generation or dissipation. The proposed approach explicitly accounts for the inter- and intra-pellet resistances to heat transfer in packed beds comprising two different types of pellets and can be further extended to model complex systems involving simultaneous reaction and adsorption.

2. METHODOLOGY

The method utilised is entirely computational. Two mathematical representations are developed: distributed and lumped parameter models. Both models are solved numerically by developing in-house solutions by finite difference approximations using Matlab™, and also, by applying the method of lines and generating simulations by gPROMS™.

3. MODEL

The investigated system consists of a cylindrical vessel randomly packed with a mixture of two types of pellets exhibiting different refractory properties and exchanging heat with a flowing stream of gas. Figure 1 depicts schematically the system to be modelled.

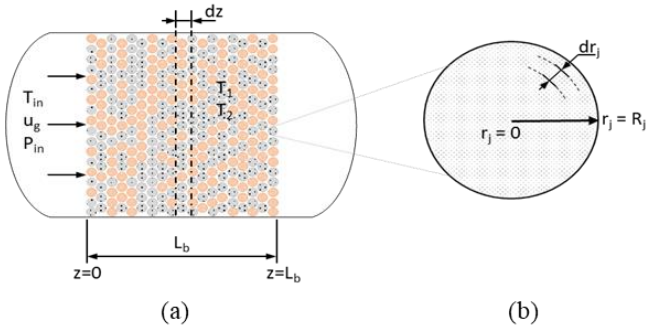

Figure 1: Schematic representation of a packed bed with two different packings indicating the domains of interest at: (a) the packed bed level and (b) the particle level.

The assumptions specified for the distributed parameter model of this heterogeneous system are: an adiabatic packed bed, plug flow, a mean bed voidage, a large bed length to diameter ratio, axial and radial thermal dispersions are negligible and all physical properties are invariant. The temperatures of

the gas T and the pellets T_i in the region of interest $t > 0, 0 \leq z \leq L_b$ and $0 < r_i < R_i$, where i = 1 or 2 are mathematically represented as follows:

$$\varepsilon_b \rho_g C_{p,g} \frac{\partial T}{\partial t} + u_g \rho_g C_{p,g} \frac{\partial T}{\partial z} = -\alpha_1 a_{S_1} \left(T - T_1|_{r_1=R_1}\right) - \alpha_2 a_{S_2} \left(T - T_2|_{r_2=R_2}\right) \tag{1}$$

The temperature within the pellets T_i are described by

$$\rho_{p_i} C_{p_i} \frac{\partial T_i}{\partial t} = \lambda_{p_i} \left(\frac{\partial^2 T_i}{\partial r_i^2} + \frac{2}{r_i} \frac{\partial T_i}{\partial r_i} \right) \tag{2}$$

with boundary conditions:

$$-\lambda_{p_i} \frac{\partial T_i}{\partial r_i}\Big|_{r_i=R_i} = \alpha_i \left(T_i|_{r_i=R_i} - T\right) \text{ and } \frac{\partial T_i}{\partial r_i}\Big|_{r_i=0} = 0 \tag{3}$$

where α_i are the heat transfer coefficients, a_{S_i} are the available areas for heat transfer per unit of volume of bed, u_g, ρ_g and $C_{p,g}$ are the gas superficial velocity, the density and the specific heat capacity, respectively, ρ_{p_i}, C_{p_i} and $\lambda_{p_i}$are the combined gas and solid densities, specific heat capacities and thermal conductivities of the pellets, respectively.

The surface areas a_{S_i} are defined as:

$$a_{S_i} = \frac{6\gamma_i(1 - \varepsilon_b)}{d_{p,i}} \tag{4}$$

where γ_i are the volumetric fractions of the pellets within the bed, ε_b is the mean voidage of the bed and $d_{p,i}$ are the diameters of equivalent volume spherical pellets.

Equations (1) – (4) are solved for a square-step forcing function; the initial state of the system is that of a thermal equilibrium between the pellets and the gas, these conditions are represented as:

$$T(0,t) = T_{in} \text{ and } \quad T(x,0) = T_i(x, r_i, 0) = T_0 \tag{5 \& 6}$$

An equivalent pseudo-homogeneous (lumped parameter) representation is obtained from equations (2) and (3) by introducing average temperatures $\tilde{T}_i$ for the pellets defined as follows:

$$\tilde{T}_i = 3 \times \left(\int_0^{R_i} T_i(r) r^2 \, \mathrm{d}r \right) / R_i^3 \tag{7}$$

The temperatures for each packing are now given by

$$\rho_{p_i} C_{p_i} \frac{\partial \tilde{T}_i}{\partial t} = \frac{3\alpha_i}{R_i} \left(T - T_i|_{r_i=R_i}\right) \equiv \alpha_i a_{S_i} \left(T - T_i|_{r_i=R_i}\right) \tag{8}$$

For the lumped model, the surface pellet temperatures $T_i|_{r_i=R_i}$ in equations (1) and (8) are replaced by average pellet temperatures $\tilde{T}_i$, which implies very small Biot numbers, $\mathrm{Bi}_i = 2\,\alpha_i R_i / \lambda_{p_i}$ equivalent to combinations of large values of the thermal conductivity, small packing sizes and small heat transfer coefficients. The pseudo-homogeneous (lumped) model is represented by modified forms of equations (1) and (8) along with equations (4), (5) and (6). This set of equations is equivalent to the well-known Schumann model, but with two different packings [5].

The model equations (1), (2) and (8) presented are transformed from the Eulerian to the Lagrangian co-ordinates by the following transformation:

$$\tau = t - \frac{z}{u_i} \tag{9}$$

The fluid energy conservation equation equation (1) is now represented in Lagrangian co-ordinates as:

$$u_g \rho_g C_{p,g} \frac{\partial T}{\partial z} = -\alpha_1 a_{S_1}\left(T - T_1|_{r_1=R_1}\right) - \alpha_2 a_{S_2}\left(T - T_2|_{r_2=R_2}\right) \tag{10}$$

and time t is replaced in equations (2), (5) and (8) by τ, which is defined as the Eulerian time minus the residence time of the gas within the bed in the transformation equation (9).

3.1 Model solution

Both the heterogeneous and pseudo-homogeneous models are solved numerically. The Lagrangian form of equation (10) is approximated by a 2nd order central difference approximation in both solutions and equations (2) for the heterogeneous solution by the fully implicit backward (FIB) finite difference scheme. Similarly, the two equations (8) for the pseudo-homogeneous solution also represented by a 2nd order central difference approximation. These numerical schemes are extensions to those presented by Handley and Heggs [6], but only details of the heterogeneous solution are presented, because in the present work the FIB numerical scheme has replaced the original Crank-Nicolson approximation [6] for equation (2).

The computational domain of the heterogeneous problem is represented by a three-dimensional (3D) mesh, which is subdivided into three separate domains namely: a plane defined by the axis $N - I$ which physically represents the space-time region bounded by the period time τ and the bed length L, and the 3D regions formed by the axis $N - I - M$ and $N - I - P$, which incorporate the space region for each pellet radius r_1 and r_2. In these coordinated systems, N is the number of nodes for the time period and I is the number of nodes along the bed length, and M and P are the number of nodes within each radius of the pellets 1 and 2 respectively.

The solution for the gas temperature T_i^{n+1} at each node of the plane $N - I$ proceeds simultaneously with the solution for the solid temperatures ${T_1}_j^{n+1,i}$ and ${T_2}_k^{n+1,i}$ at the nodes of each row in the regions bounded by the axes $N - I - M$ and $N - I - P$; where the superscripts n, i represent the time and length coordinates of the gas and solid temperatures within the computational mesh, and the subscripts j, k represent the spatial coordinates of the solid temperatures nodes.

By applying the second order central differences discretisation to equation (10), the following algebraic expression is obtained:

$$\begin{aligned} -A_1 {T_1}_m^{n+1,i} + [2 + A_1 + A_2] T_i^{n+1} - A_2 {T_2}_p^{n+1,i} \\ = [2 - A_1 - A_2] T_{i-1}^{n+1} + A_1 {T_1}_m^{n+1,i-1} + A_2 {T_2}_p^{n+1,i-1} \end{aligned} \tag{11}$$

where ${T_1}_m^{n+1,i}$, ${T_1}_m^{n+1,i-1}$, ${T_2}_p^{n+1,i}$ and ${T_2}_p^{n+1,i-1}$ are the temperatures on the surfaces of the pellets, and A_1, A_2 are solution constants dependent upon the fluid and particle properties, the heat transfer coefficient, the axial step-size Δz, and their definitions are:

$$A_1 = \frac{\alpha_1 a_{S_1} \Delta z}{u_g \rho_g C_p} \text{ and } A_2 = \frac{\alpha_2 a_{S_2} \Delta z}{u_g \rho_g C_p} \tag{12}$$

Equation (2) is discretised for each particle by the FIB discretisation scheme - the backward discretization of the time derivative and the application of central differences to the spatial derivative at the time $n+1$, yielding the following algebraic equation applicable to the interior nodes of each pellet, so i = 1 or 2 in the following set of equations:

$$-\left(1+\frac{1}{k_i}\right) M_i T_{i_{k_i+1}}^{n+1,j} + (1+2M_i) T_{i_{k_i}}^{n+1,j} - \left(1-\frac{1}{k_i}\right) M_i T_{i_{k_i-1}}^{n+1,j} = T_{1_{k_i}}^{n,j} \tag{13}$$

At the centre of the pellet the application of the symmetry condition in equation (3) produces the following algebraic equation:

$$-6M_i T_{i_1}^{n+1,j} + (1+6M_i) T_{i_0}^{n+1,j} = T_{i_0}^{n,j} \tag{14}$$

whereas at the surface of the particle, the boundary condition at $r_i = R_i$ expressed in equation (3) is approximated by central difference formula and then combined with equation (13) at the surface to eliminate a fictitious node outside the region of interest to provide the following equation:

$$-\left(1+\frac{1}{m_i}\right) C_i M_i T_i^{n+1} + \left[1 + M_i\left(2+\left(1+\frac{1}{m_i}\right) C_i\right)\right] T_{i_{m_i}}^{n+1,j} - 2M_i T_{i_{m_i-1}}^{n+1,j} = T_{i_{m_i}}^{n,j} \tag{15}$$

where M_i are functions of both the fluid and the packings' properties, as well as of the step-sizes for time $\Delta\tau$, axial space Δz and radial space Δr_i, where $i = 1,2$ depending on the type of packing and are defined as follows:

$$M_i = \frac{\lambda_{p_i}}{\rho_{p_i} C_{p_i}} \frac{\Delta\tau}{(\Delta r_i)^2} \tag{16}$$

The equations (11), (13), (14) and (15) form a linear system of equations $Ax = b$, where A is a tridiagonal matrix, x is a vector of the unknown temperatures and b is a vector of known temperatures. The unknown temperatures are obtained by employing the Thomas algorithm. The pair of numerical schemes and their solutions were developed and implemented in Matlab™, and also, solutions were developed and obtained using the method of lines in the gPROMS™ software.

4. RESULTS

4.1 Convergence of the solution.

The convergence of the proposed numerical solution was analysed by varying the number of mesh nodes within the spatial coordinates (nr_1, nr_2 and nz) at a fixed time step-size of $\Delta\tau = 0.1$s and observing the deviation of the output from the solution obtained from gPROMS™. The computational experiments for the convergence analysis were run for a mixture of alumina and calcium oxide packings of equal size (0.0092m) with $\gamma_1 = 0.25$ and $\gamma_2 = 0.75$, where γ_i represents the volumetric fraction of of a packing in the bed. The studied system was a packed bed of 1 m in length exchanging heat with a hot gas stream with mass flux $G = 7.61\ \text{kg m}^{-2}\text{s}^{-1}$ and heat capacity $C_{p_g} = 2597.7\ \text{J kg}^{-1}\text{K}^{-1}$; the packings properties and other parameters utilised in the simulations are summarised in Table 1.

Figure 2(a) and (b) illustrate the evolution of the breakthrough when the number of points utilised to discretise the bed length and the particles' radii are set to 5, 10, 20 and 50. To conduct the exercise the number of points of the three spatial domains was set to be equal. It is remarkable how fast the numerical scheme seems to converge to the solution from gPROMS™; by setting nr_1, nr_2 and nz to 20

the solution exhibits an average error ranging from 0.686% to 0.691% for the case of 25%v/v of alumina in the packed bed and ranging from 0.603% to 0.607% for the case of 75%v/v of alumina in the mixture of packings; this confirms that the proposed scheme is stable and convergent, and in fact very competitive considering that the time step-size was not optimised as opposed to the way gPROMS™ handles its algorithm.

Table 1. Simulation parameters utilised in all computational experiments in this investigation.

Packing	ρ_{p_i} $(kg\ m^{-3})$	C_{p_i} $(J\ kg^{-1}K^{-1})$	λ_{p_i} $(J\ m^{-1}s^{-1}K^{-1})$	α_i $(J\ m^{-2}s^{-1}K^{-1})$	a_{S_i} (m^2m^{-3})	γ_i (m^3m^{-3})	ε_b (m^3m^{-3})
Alumina	3630	1240.7	2.1	1366.8	409.8	0.25/0.75	0.37
Calcium Oxide	3340	943.4	8.5	1366.8	409.8	0.75/0.25	0.37

The average error was calculated based on the actual value of the gas breakthrough temperature to avoid the magnification of the error magnitude due to the small values of the dimensionless temperature; the following formula was applied:

$$Error = \frac{1}{n}\sum_{n=1}^{k}\left(1 - \frac{T_{FIB}}{T_{gPROMS}}\right) \tag{17}$$

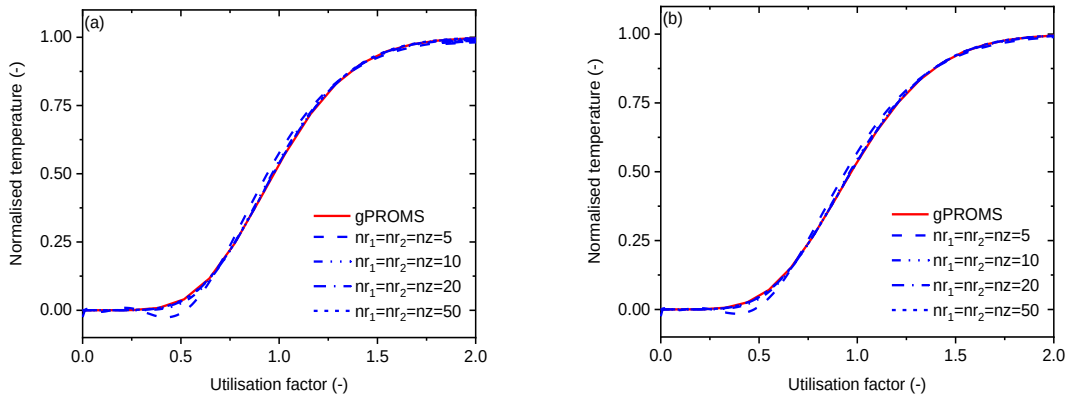

Figure 2: (a) Convergence of the FIB numerical scheme for packed bed with 25%v/v of alumina and 75%v/v of calcium oxide. (b) Convergence of the FIB numerical scheme for packed bed with 75%v/v of alumina and 25%v/v of calcium oxide.

4.2 Application of the model to simulate the heating of a fixed bed packed with mixtures of refractory packings.

The model was utilised to simulate the heat transfer in several packed beds with different volumetric fractions of packing types 1 and 2. Figure 3(a) is a plot of the breakthrough curves obtained with the heterogeneous model in dimensional form for each of the cases simulated; for comparison purposes the output of the pseudo-homogeneous model is also plotted. It is evident from Figure 3(a) that the effect of the volumetric fraction of alumina on the breakthrough curve is twofold, on one hand, augments the time required to saturate the bed to the temperature of the incoming gas. On the other hand, a higher degree of dispersion is observed as the presence of this material in the packed bed increases. Figure 3(b) is a plot of the temperature profiles of the packing types 1 and 2 as function of time and axial position for a 50%/50% mixture of alumina and calcium oxide spherical packings. Since both materials have been assumed to have the same size, they exhibit the same heat transfer area and heat transfer coefficient, however, the alumina packings exhibit a higher density than the calcium oxide ones. Hence, Figure 3(b) reflects how the less dense material will reach the saturation temperature first.

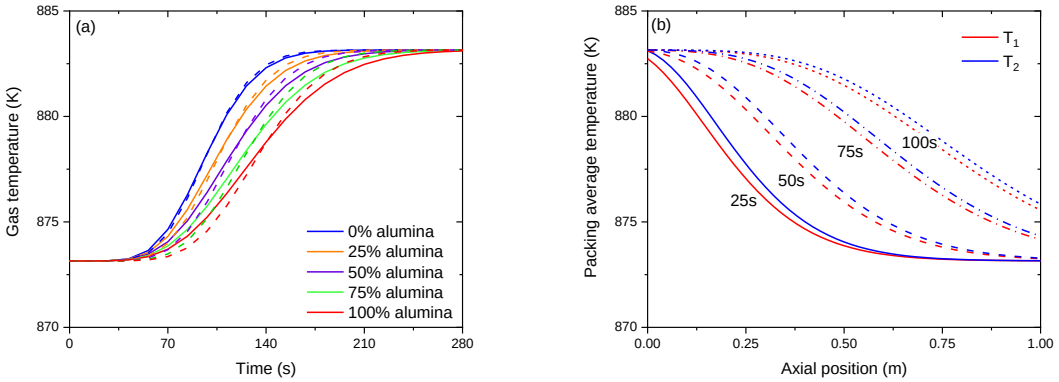

Figure 3: (a) Breakthrough curves in dimensional form of various fixed beds packed with different volumetric fractions of a mixture of alumina and calcium carbonate pellets (solid line: heterogeneous model; dashed line: pseudo-homogeneous model). (b) Temperature profiles of the alumina (T_1) and the calcium oxide (T_2) packings for a 50%/50% mixture at various simulation times.

5. CONCLUSIONS

The heat transfer between a hot gas stream and a packed bed formed by two types of refractory packings has been investigated. Heterogeneous and pseudo-homogeneous models are presented. Convergent, compatible and stable numerical solutions are developed and implemented in Matlab™. The models are validated by comparison with results using the method of lines in the gPROMS™ software and used to analyse the heat transfer response of various packed beds with different contents of packing type 1 (Al_2O_3) and type 2 (CaO). The increase of alumina packings in the packed bed augments the intra-conduction effects and the time of saturation of the bed. Hence the heterogeneous model should be applied to ensure the estimation of the transients and saturation time and is recommended for investigations of catalytic packed bed reactors with in-situ adsorption pellets.

ACKNOWLEDGEMENTS

Erik Resendiz-Mora acknowledges the financial support from Conacyt-SENER and SEP.

REFERENCES

1. Xu, B., P.W. Li, and C.L. Chan, *Extending the validity of lumped capacitance method for large Biot number in thermal storage application.* Solar Energy, 2012. **86**(6): p. 1709-1724.
2. Sadrameli, S.M. and H.R.B. Ajdari, *Mathematical modelling and simulation of thermal regenerators including solid radial conduction effects.* Applied Thermal Engineering, 2015. **76**: p. 441-448.
3. Abbas, S.Z., V. Dupont, and T. Mahmud, *Modelling of high purity H2 production via sorption enhanced chemical looping steam reforming of methane in a packed bed reactor.* Fuel, 2017. **202**: p. 271-286.
4. Diglio, G., et al., *Modelling of sorption-enhanced steam methane reforming in a fixed bed reactor network integrated with fuel cell.* Applied Energy, 2018. **210**: p. 1-15.
5. Schumann, T.E.W., *Heat transfer: A liquid flowing through a porous prism.* Journal of the Franklin Institute, 1929. **208**: p. 405-416.
6. Handley, D. and P.J. Heggs, *Effect of Thermal Conductivity of Packing Material on Transient Heat Transfer in a Fixed Bed.* International Journal of Heat and Mass Transfer, 1969. **12**(5): p. 549-570.